Searching for Neurophysiological Biomarkers Correlated with BCI Performance in a Completely Locked-In State Patient

Rute Bettencourt
Institute of Systems and Robotics - University of Coimbra
Portugal
rute.bettencourt@isr.uc.pt

Urbano J. Nunes
Institute of Systems and Robotics - University of Coimbra
Portugal
Department of Electrical and Computer Engineering - University of Coimbra
Portugal
urbano@isr.uc.pt

Miguel Castelo-Branco
Coimbra Institute for Biomedical Imaging and Translational Research - University of Coimbra
Portugal
Faculty of Medicine - University of Coimbra
Portugal
mcbranco@fmed.uc.pt

Gabriel Pires
Institute of Systems and Robotics - University of Coimbra
Portugal
Polytechnic Institute of Tomar
Portugal
gpires@isr.uc.pt

Abstract

Patients in a completely locked-in state (CLIS) lose the ability to control all voluntary muscles, including eye-movements. Although they remain aware of their surrounding environment, they are unable to communicate. Brain-computer interfaces (BCIs) offer the last resort for communication by using brain signals to establish a direct channel between the brain and an external device such as a computer. However, achieving effective BCI communication with CLIS patients has proven very challenging. In a previous study, we conducted experiments over ten months with a CLIS patient showing significant variability in BCI performance over sessions. This variability can stem from multiple factors including fluctuating levels of arousal, consciousness and vigilance, which are difficult to directly assess in the patient. In this study, using the data collected over the ten months, divided into good and poor performance sessions/epochs, we search for neurophysiological biomarkers that could correlate with the BCI performance variability. Several frequency domain metrics are tested, such as power spectral density (PSD), the power law exponent (PLE), the delta-alpha ratio (DAR), and the power ratio index (PRI). Results indicate statistical differences between the two conditions (good vs poor BCI performance) in the PLE index (p<0.05 in the Wilcoxon rank sum test). Additionally, exploratory tests with a convolutional neural network, EEGNet, showed the potential to discriminate good and poor performance with a balanced accuracy of 84.1%. The overall results are relevant for determining the optimal times for a patient to use BCI, thereby enhancing communication efficacy.

DSAI 2024, November 13–15, 2024, Abu Dhabi, United Arab Emirates

ACM ISBN 979-8-4007-0729-2/24/11
https://doi.org/10.1145/3696593.3696611

CCS Concepts

• **Human-centered computing** → **Human computer interaction (HCI)**; • **Applied computing** → **Life and medical sciences**; • **Computing methodologies** → *Machine learning*.

Keywords

Brain-computer interface, Completely locked-in state, Electroencephalography, Vigilance, Arousal, Power spectral density, Delta-alpha ratio, Power ratio index, Power-law exponent, EEGNet

ACM Reference Format:
Rute Bettencourt, Urbano J. Nunes, Miguel Castelo-Branco, and Gabriel Pires. 2024. Searching for Neurophysiological Biomarkers Correlated with BCI Performance in a Completely Locked-In State Patient. In *11th International Conference on Software Development and Technologies for Enhancing Accessibility and Fighting Info-exclusion (DSAI 2024), November 13–15, 2024, Abu Dhabi, United Arab Emirates.* ACM, New York, NY, USA, 8 pages. https://doi.org/10.1145/3696593.3696611

1 Introduction

Patients in the completely locked-in state (CLIS), either due to stroke or neurodegenerative diseases such as amyotrophic lateral sclerosis (ALS), are unable to volitionally control their movements. While patients in late stages of ALS including those in locked-in state (LIS) are still able to use eye tracking technology to communicate, they lose this ability when entering CLIS. Brain-computer interfaces (BCIs) attempt to bypass the usual neuronal motor pathways by interpreting brain signals acquired through methods such as electroencephalography (EEG) or intracortical implants, thereby creating an alternative communication system via a computer. BCIs have been applied to patients in CLIS; however, a continuous, reliable communication channel for these patients is yet to be established (see [4, 12] as examples of moderate success).

Martens et al [11] suggest that patients in CLIS may suffer from declining awareness and have episodes of low arousal. These alterations could be the cause of the lack of BCI control by this clinical

population. Wu et al [16] performed a multiscale approach analysis of consciousness in a CLIS patient. By applying a multiscale sample entropy, multiscale permutation entropy, and multiscale Poincaré plots to electrocorticogram signals, the authors showed the possibility of correctly identifying periods of consciousness. Other studies show the altered and fluctuating levels of arousal and their implications for the difficulty in establishing communication with CLIS patients [1, 17].

In our previous study [2], a patient in CLIS was followed over a period of ten months conducting 31 sessions. During this period, nine BCI variants were tested in an attempt to establish communication with the patient. The BCI performance showed significant variability over sessions even when the same variant of the BCI was used, and a great variability of responses to stimuli within the same session. This led us to conclude that BCI performance has been greatly affected by patient's mental state possibly related to attention and arousal at the time of operating the BCI.

The current study aims to assess whether it is possible to identify neurophysiological biomarkers that can be correlated to BCI performance. To do this, a frequency analysis was conducted, using quantitative EEG metrics that may characterize altered EEG rhythms related to attention and arousal [14, 16] during sessions where BCI performance was worse. Additionally, a convolutional neural network, EEGNet, was used in an agnostic manner, enabling the model to independently identify patterns and features. This approach was used to assess the feasibility of predicting good vs poor performance.

2 Methods

2.1 Participants and recorded datasets

The analysis performed in this study uses data from our previous study [2], which involved testing nine BCI variants with different visual, audio and hybrid visuo-auditory stimuli on a single CLIS patient over a period of ten months. The participant was a 54-year-old female CLIS patient with ALS, with a functional rating scale-revised (ALSFRS-R) score of 1. In the initial experiments, the patient had no eyelid movement control nor vertical movement control, possessing only a slight horizontal eye movement which she used to communicate 'Yes' responses. She lost this remaining ability a couple of months after the initial experiments. For comparison, three of the BCIs were also tested by a control group of 5 able-bodied participants. For detailed information, see [2].

The EEG data was acquired with a 16-channel g.USBamp acquisition device (g.tec medical engineering GmbH, Schiedlberg, Austria) at a sampling rate of 256 Hz from 16 g.Ladybird electrodes (Fz, Cz, C3, C4, CPz, Pz, P3, P4, PO7, PO8, POz, Oz, FPz, FCz, FC1, and FC2) placed according to the extended international 10-20 system. The signals were filtered by a band-pass filter between 0.1 and 30 Hz and a notch filter at 50 Hz to eliminate the powerline interference. Data were acquired, processed, and classified in real-time in a Highspeed online processing Simulink framework.

For the current study, the recorded calibration datasets were separated into two datasets: datasets related to good BCI performance, defined as those which had an online classification accuracy of 70% or above, and poor performance datasets, which had an online classification accuracy of less than 70%. Overall, there were 7 BCI sessions with good performance and 18 sessions with poor BCI performance. The EEG data were further filtered using a 4th-order Butterworth high-pass filter, with 0.5 Hz cut-off frequency as artifact components were found below this frequency.

2.2 BCI paradigms

The BCI paradigms consisted of visual, audio and hybrid interfaces based on the P300 event-related potential. Each interface consisted of 7 Portuguese words that related to the patient needs (see Figure 1, where the word 'STOP' is overlapped by the face stimulus). The visual component suffered iterative designs until a grid layout (two lines, four columns) was achieved. Each cell of this grid had one of the Portuguese words written. The stimulus to select the word was either a male face, as shown in Figure 1, overlapping the word or a face of a family member of the patient. The audio components were the spoken version of the 7 Portuguese words [1]. Although having 7-symbols, only Yes and No could be selected, which was made to improve BCI communication feasibility. See details in [2].

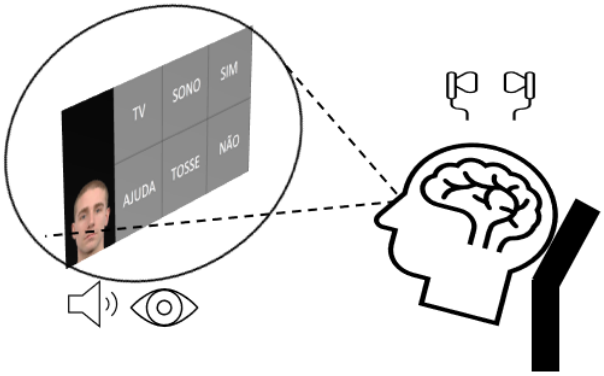

Figure 1: Visual component of the standard face interface tested with the patient and the control group. Participants were instructed to mentally count the number of times the face blinked over the desired word. During the hybrid interface, the words were presented to the participants via the computer screen (visual component) and earphones (audio component).

2.3 Neurophysiological metrics

The neurophysiological analysis focused on frequency features where it is expected to contain information related to arousal, such as the delta-alpha ratio (DAR), and the power ratio index (PRI), which indicate the relationship between the slow and fast frequencies and are commonly used in outcome prognosis prediction in hemorrhagic stroke patients [7–9]. Moreover, the power-law exponent (PLE) was included to reflect the non-periodic broadband nature of EEG signals, which has been used as a biomarker to detect levels of consciousness [5, 17]. These metrics were applied to the

[1] See demonstrative videos at https://home.isr.uc.pt/~gpires/videos/BCI4ALL/videos.html

continuous EEG signal of the recorded datasets for the two conditions: good vs poor BCI performance. The first step was applying the Welch method to the continuous EEG signal to obtain a reliable power spectral density (PSD) estimation. The obtained PSD was then used for computing the subsequent metrics presented in this study.

The Welch method was applied by segmenting the time-series in M Hanning windows of $N = 256$ time-samples of length, with a 50% overlap. The number of points for the FFT (NFFT) was 256 (the same of N) and the sampling rate was 256 Hz, leading to a frequency resolution of 1 Hz. The PSD of an EEG signal x is estimated from the average M modified periodograms, x_m:

$$PSD(x) \equiv \widehat{S}_x(k) = \frac{1}{M} \sum_{m=0}^{M-1} P_{x_m}(k), k = 1..NFFT - 1 \quad (1)$$

with

$$P_{x_m}(k) = \frac{1}{NFFT} |FFT(x_m)|^2 \quad (2)$$

From visual inspection of the resulting spectra, noisy channels were removed from the data to avoid biasing the analysis. The power spectral densities were further divided into delta (1-4 Hz), theta (4-8 Hz), alpha (8-13 Hz), and beta (13-30 Hz) frequency bands to compute the delta-alpha ratio (DAR) and the power ratio index (PRI). The power law exponent (PLE) was computed using the PSD data between 1 and 30 Hz. These metrics are presented in the following sections. The differences between good and poor performance conditions were then statistically evaluated by applying the Wilcoxon rank sum test.

2.3.1 Power law exponent. The power law exponent (PLE) also known as the spectral exponent [6] is a measure of the variation of the power spectrum across frequencies. It is known that the aperiodic brain activity follows a distribution given by $1/f^{\beta}$, where β is a characteristic parameter of brain activity. This parameter is easily calculated from the slope of the PSD when represented in log-log space. The spectral exponent (β) is obtained as follows:

$$log(PSD(f)) = log(\frac{1}{f^{\beta}}) = -\beta log(f) \quad (3)$$

$$\beta = -\frac{log(PSD(f))}{log(f)} \quad (4)$$

The β-PLE is obtained by applying a linear least squares regression to the PSDs of the EEG data. This β-PLE provides the slope of the PSD and helps interpret the overall PSD behavior, as it is computed from the entire EEG frequency range.

2.3.2 Delta/alpha ratio. The delta/alpha ratio (DAR) [7] is used to assess the degree of EEG slowing. DAR is known to decrease in elderly population and people with neurological disorders. It is calculated from:

$$DAR = \frac{r\delta}{r\alpha} \quad (5)$$

where rδ is the relative power of the delta band, obtained by dividing the average power in the delta frequency band by the average power between 1 and 30 Hz, and rα is the relative power of the alpha band, obtained by dividing the average power in the alpha frequency band by the average power between 1 and 30 Hz.

2.3.3 Power ratio index. The power ratio index (PRI) [3] (also named as (delta + theta)/(alpha + beta), DTABR) evaluates the ratio between slow and fast EEG waves following the expression:

$$PRI = \frac{r\delta + r\theta}{r\alpha + r\beta} \quad (6)$$

with $r\delta$, $r\theta$, $r\alpha$, $r\beta$ being the relative power between the different frequency bands, obtained by dividing the frequency band's absolute power by the total power (1 to 30 Hz).

2.4 Automatic Prediction of BCI Performance with EEGNet

To investigate the feasibility of automatically predicting patient BCI performance, we employed EEGNet [10], a well-established convolutional neural network (CNN) designed for EEG classification. EEGNet is specifically structured to extract both temporal and spatial features from EEG data, consistent with the conventional pipeline for EEG classification [13]. The data is input as raw data after normalization to zero mean and standard deviation of 1 (z-score). EEGNet was used without prior assumptions about which specific features might be relevant for predicting BCI performance. Instead, EEGNet was 'allowed' to identify patterns and features on its own, without bias towards any particular set of features.

Using the same datasets used for neurophysiological analysis, categorized into good BCI performance and poor BCI performance, the data from non-target events was selected, excluding P300 target events to ensure that predictions were influenced solely by ongoing EEG activity. In total, the good performance data consisted of 4536 non-target epochs, while the poor performance data comprised 14904 non-target epochs. Each EEG epoch had dimensions of $N_{ch} \times T_{samp}$, where N_{ch} represents the number of EEG channels (16) and T_{samp} denotes the number of samples per EEG epoch (256 samples, corresponding to one second).

3 Results

Twenty-five datasets (each one corresponding to one session) from the CLIS patient were analyzed. Seven datasets correspond to the good performance condition and the remaining eighteen correspond to the poor performance condition. For the control group (15 datasets, three from each participant), there was no division between good and poor performance since all the sessions with healthy participants had online classification accuracies above 70% (online averages were 88.0%, 92.0%, 98.0%, for the three tested BCI variants). Power spectral density analysis, power law exponent analysis, delta-alpha ratio and power ratio index analysis were performed.

3.1 Neurophysiological comparison between good and poor performance

In this section, the different neurophysiological metrics proposed in the methods' section were analyzed. The results for the good performance condition (sessions with online classification accuracy above 70%) were compared with the results from the poor performance condition.

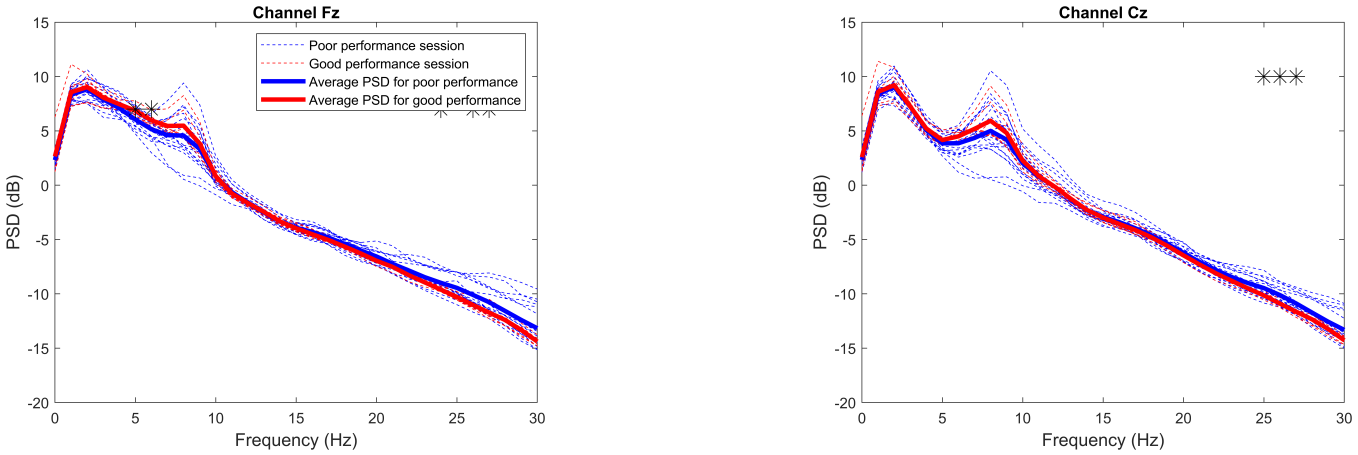

Figure 2: Power spectral density of the CLIS patient obtained from electrode (a) Fz, and (b) Cz. The stars * indicate the frequency ranges where statistically significant differences between good and poor performance conditions were found (p<0.05 in the Wilcoxon sum rank test).

3.1.1 PSD comparison. The Welch PSD was obtained for all channels and sessions. The results from channels Fz and Cz are represented in Figure 2a and 2b, respectively. There is a peak in power around 7 Hz for all channels. Channel Fz shows statistically significant differences between the two conditions in the theta and beta bands (p<0.05 in the Wilcoxon rank sum test). In PO7, a statistical difference is found only in the theta band. Channels C3, CPz, Cz, FC1, FPz, Oz, P4, and POz, presented statistical differences in the beta band. No statistically significant differences were found in the remaining channels.

3.1.2 Power band comparison. The PSDs obtained for both good and poor BCI performances were divided into the delta, theta, alpha, and beta frequency bands. The values within each band were averaged to obtain the average power band. Figure 3 shows the average power band for the two conditions at electrodes in the central region (C3, C4, CPz, and Cz). Our analysis did not reveal statistically significant differences between the good and poor performance groups for any combination of channel-frequency band (p<0.05 in the Wilcoxon rank sum test), although a tendency towards higher average power in central electrodes for the good performance condition can be observed in Figure 3.

3.1.3 PLE comparison. The β-PLE was calculated for each channel. The distribution of PLE values was evaluated for good and poor performance, first for each individual channel and then by combining the values from all electrodes. The distribution results for all channels are presented in Figure 4a. The median β-PLE values were 1.74 for good performance and 1.65 respectively poor performance. Statistically significant differences were found between the two conditions when considering the combination of all electrodes. When evaluating channels individually, the median values of PLE for the good performance condition were higher than for the poor performance, but these channel-by-channel differences were not statistically significant.

3.1.4 DAR comparison. Similarly to the previous approach, the DAR was computed first for each channel and then across all channels. The median DAR value for the good performance group considering all channels was 2.99, whilst the median value for the poor performance group was 3.12, although no statistically significant differences were found between the two conditions (p<0.05 in the Wilcoxon rank sum test). The results are depicted in Figure 4b. The channel-by-channel approach also did not show significant differences between the two conditions.

3.1.5 PRI comparison. The comparison between good and poor performance conditions was computed for each individual channel and then across all channels. The results are presented in Figure 4c. The median value of the PRI for the good performance and poor performance were respectively 4.37 and 4.08, yet no statistical significances were found.

3.2 Neurophysiological comparison between patient and control group

For the neurophysiological comparison between patient and control group, the patient's good and poor performance data were combined and then compared to the control group's data (all good performance). The results are displayed in Figure 5. We found that the PSD was higher in the control group, with statistical differences for all frequency bands except for the alpha band (p<0.05 in the Wilcoxon rank sum test). The β-PLE was lower in the control group than in CLIS, with statistically significant differences in channels C3, C4, Cz, FC1, FC2, FCz, Fz, and P3 (p<0.05 in the Wilcoxon rank sum test), indicating a steeper slope of the $1/f^{\beta}$, plot in the log-log space for the CLIS data. The DAR is lower in the CLIS patient across all channels, with significant differences found in channels CPz, Cz, FC1, FC2, FCz, FPz, Fz, P3, P4, PO8, and Pz (p<0.05 in the Wilcoxon rank sum test). This result aligns with the PSD analysis, where a decrease in delta band power was identified, while the alpha power remained similar to that of healthy participants. Lastly, the PRI was

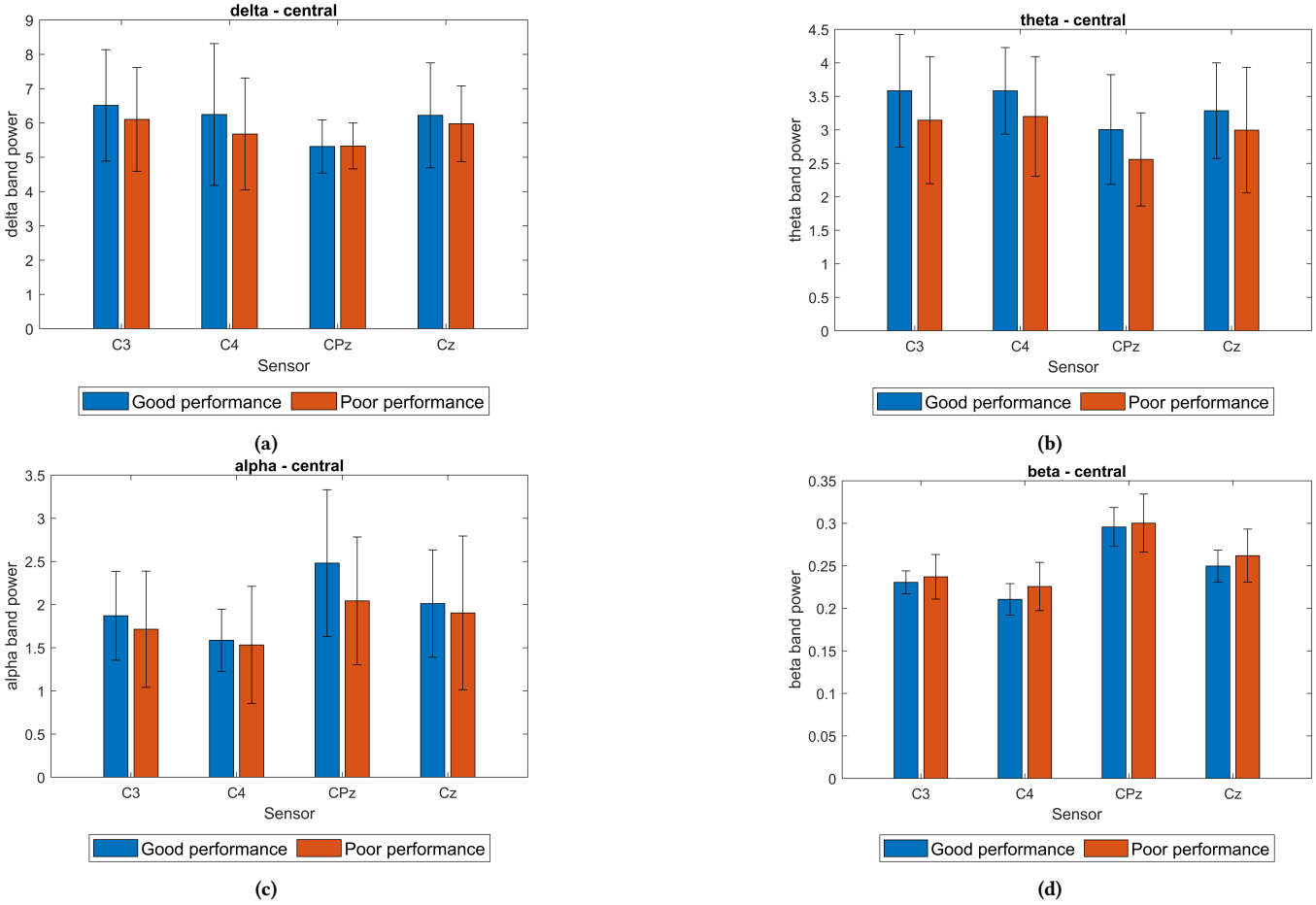

Figure 3: Band powers of the CLIS patient obtained at the central region (in electrodes C3, C4, CPz, Cz) for the (a) delta, (b) theta, (c) alpha, and (d) beta bands. No statistical differences were found between the good performance group and the poor performance group (p<0.05 in the Wilcoxon sum rank test).

also lower in the CLIS patient across all channels, with significant statistical differences being found in channels Cz, FC1, FCz, FPz, and Fz (p<0.05 in the Wilcoxon rank sum test). From these results, it can be inferred that most of the differences between the control group and the CLIS patient occur in the frontal and central brain regions.

3.3 EEGNet Prediction Results

EEGNet was used to investigate the feasibility of automatically predicting patient BCI performance by discriminating between good and poor performance. The dataset, consisting of 4536 samples for good performance and 14904 samples for bad performance, as described in Section 2.4, was randomly split into training (50%), validation (25%) and testing (25%) sets. EEGNet was trained on the training data and validated on validation data, and finally tested on unseen testing data. The model was initially trained using single EEG epochs ($N_{ep} = 1$). Subsequently, these results were compared with those obtained from combining multiple EEG epochs, specifically 3, 6 and 54 epochs. The combination involved concatenating the epochs in the time dimension. For 6 epochs, this was equivalent to a complete trial (as the BCI paradigm includes 7 symbols: 1 target and 6 non-targets), and 54 epochs correspond to a full trial of 9 repetitions (9×6), which were used during online operation and calibration. Due to the class imbalance, the results are reported in terms of balanced accuracy, precision, recall and F1 scores (see Table 1). The best balanced-accuracy result was 84.1% with a precision of 93.4% for one EEG epoch. EEGNet achieved worse results for a larger number of concatenated epochs indicating difficulty in handling the high input dimension. For example, for the concatenation of 54 epochs, the EEG input dimension was 16×13824 where 13824 corresponds to 54×256 time samples. The models were trained on an NVIDIA GeForce RTX 3060, with CUDA 11.2 and cuDNN 8.1.0, using Tensorflow and the Keras API.

4 Discussion

In this study, we analyzed data recorded from a CLIS patient while controlling a BCI over a period of 10 months. Given the significant variability of BCI performance across sessions and within sessions,

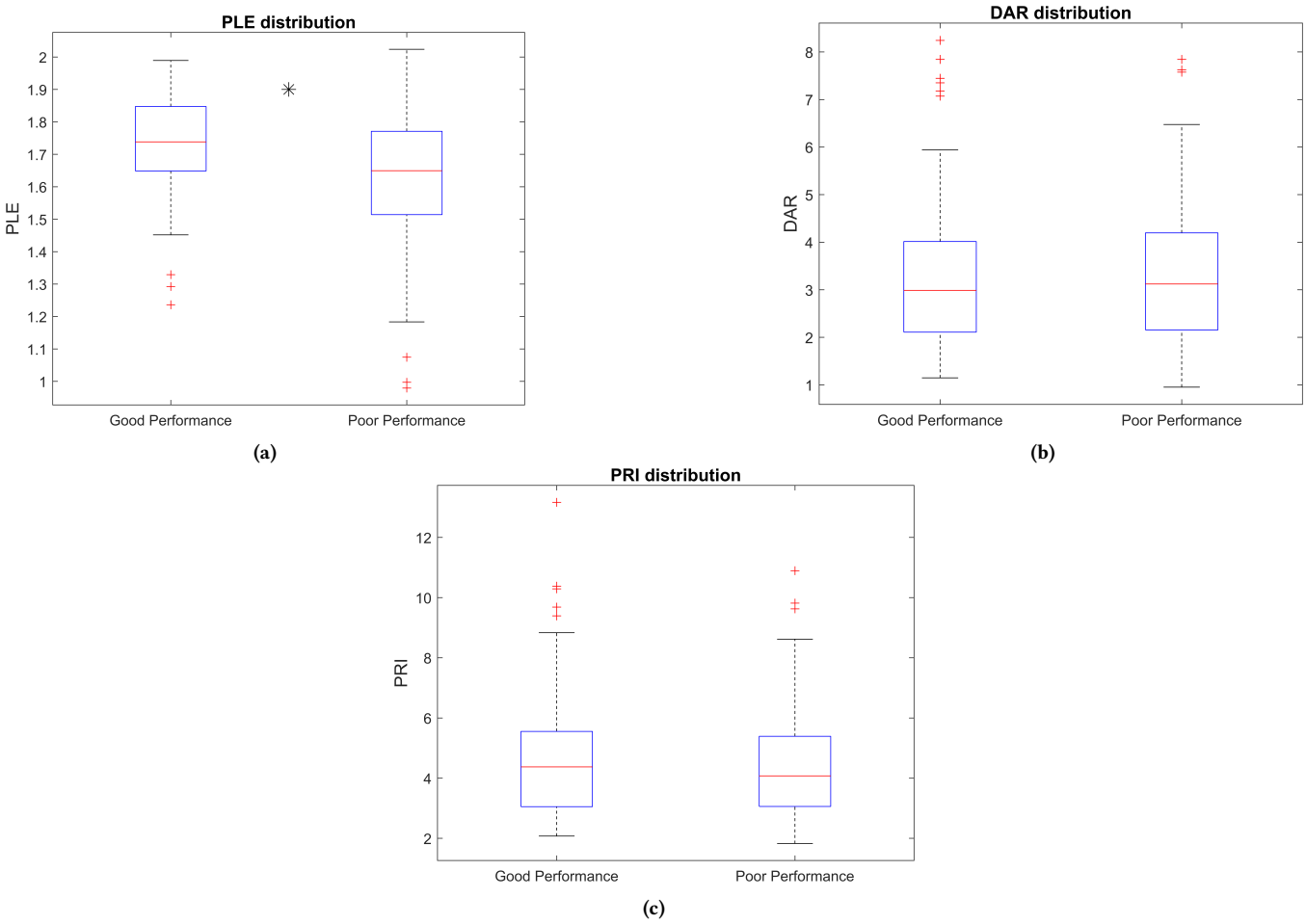

Figure 4: CLIS patient distributions for (a) PLE, (b) DAR, and (c) PRI. Statistically significant differences between good and poor performance conditions were found for PLE combining all channels (p<0.05 in the Wilcoxon rank sum test).

Table 1: EEGNet results for automatically predicting good vs poor BCI performance with different number of EEG epochs (N_{ep}).

EEG epochs (N_{ep})	Accuracy (%)	Balanced Accuracy (%)	Precision (%)	Recall (%)	F1 (%)
1	87.1	84.1	93.4	89.6	91.5
3	86.5	79.6	89.3	93.3	91.3
6 (1 round)	85.6	68.0	85.0	99.1	91.5
54 (1 trial)	80.0	75.1	86.2	86.2	86.2

we aimed to identify neurophysiological biomarkers correlated with BCI performance. Our results indicate that the PLE correlates the BCI performance outcomes, while the DAR and the PRI do not significantly change between poor and good performance conditions. We also compared the patient's EEG data with that of a healthy control group. It was observed that the patient's EEG PSDs were lower in all frequency bands except for the alpha band. The beta PLE was increased, while the DAR and PRI were lower in the patient compared to the control group.

The β-PLE was higher for the CLIS patient than for the healthy control group, which agrees with findings from [17]. That study also demonstrated higher β-PLE values during deep sleep compared to wakefulness. However, our results showed a lower β-PLE for poor BCI performance, contradicting the initial hypothesis that poor BCI performance could be related to lower vigilance and awareness levels. This may indicate that the patient was in a wakeful state. It is noteworthy that the analysis in [17] was conducted on resting state data, while ours was conducted with data collected during BCI operation, making the analyses not fully comparable. Overall, the

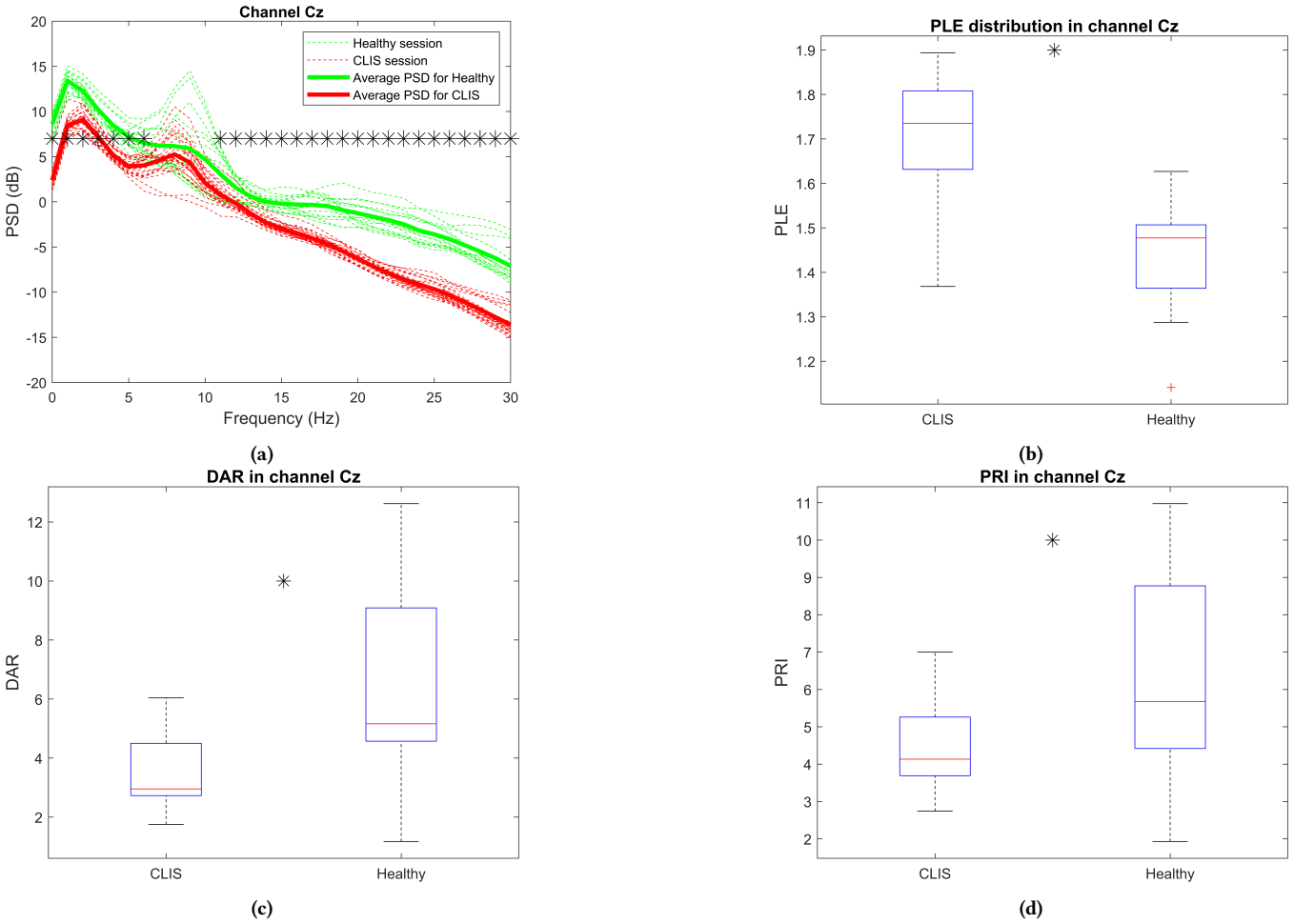

Figure 5: Control group vs CLIS patient analysis in channel Cz. a) Power spectral densities for the different sessions in dotted line and average for each group in continuous line, with statistical differences for each frequency bin signaled with *. b) Distribution of the PLE values calculated in each session. c) Distribution of DAR values calculated in each session. d) Distribution of PRI values calculated in each session.

β-PLE has proven to be a versatile metric that allows a global view of the PSD's behavior. For instance, an increase in power at slower frequencies is not mandatorily associated with a higher value of PLE, due to its dependence of the full frequency spectrum, with intermediate and higher frequencies being able to attenuate the slope associated with the β-PLE, reducing its value. EEG studies have shown EEG power decrease in CLIS patients across all frequency bands [14]. Yet, our study only confirms decreased power in the delta, theta and beta frequency bands, with alpha band power showing no statistical differences between the CLIS patient and the healthy control group. Again, these differences may be related to the fact that the mentioned study was conducted on resting-state EEG data, whereas our study was conducted on task-based BCI data, limiting direct comparison between studies.

Although the DAR and the PRI are not usually applied in CLIS patients –they are more commonly used in stroke patients as a prognostic tool [7, 9] – these metrics simply relate the different power bands, quantifying the degree of EEG slowing. There was no evidence of statistical differences in DAR and PRI between poor and good performance conditions for the CLIS patient. However, there was a significant difference in these metrics when compared to the healthy control group, indicating a lower power of the delta band for the patient.

The application of EEGNet to automatically predict good vs poor performance yielded promising results. With a balanced accuracy of 84.1% and a precision of 93.4%, the classifier effectively distinguishes between the two conditions, demonstrating high certainty in predicting good BCI performance. While these results are encouraging as they can be used to enhance real-time BCI operation, and could be used to complement the neurophysiological analysis, they should be approached with caution and further evaluation in terms of interpretability and online application is necessary.

The study was exploratory but provided insightful information that encourages us to extend it. The study was conducted with

a single CLIS patient and therefore cannot be generalized to the CLIS population. Future studies should include more patients, and explore other metrics, such as the Lempel-Ziv complexity [15, 17], or metrics based on functional connectivity analysis between the different brain regions during the BCI training task. Future analysis should also include data analysis within sessions to assess temporal fluctuation of neurophysiological states.

5 Conclusion

This exploratory study showed that β-PLE correlates with BCI performance in data acquired from one CLIS patient. It also revealed differences in the PSD of the CLIS patient compared to the healthy control group. Future work should aim to include more CLIS patients to generalize these findings. Additionally, exploring other metrics, such as dynamic functional connectivity, or Lempel-Ziv complexity, could provide insight into predicting BCI performance.

Acknowledgments

This work is financed by national funds through FCT - Fundação para a Ciência e a Tecnologia, I.P., under the projects UIDB/00048/2020 (DOI 10.54499/UIDB/00048/2020), UIDP/00048/2020, and BCI4ALL2024. Rute Bettencourt was supported by the FCT Ph.D. scholarship 2023.03995.BD (doi: 10.54499/2023.03995.BD)

References

[1] Michael Bensch, Suzanne Martens, Sebastian Halder, Jeremy Hill, Femke Nijboer, Ander Ramos, Niels Birbaumer, Martin Bogdan, Boris Kotchoubey, Wolfgang Rosenstiel, Bernhard Schölkopf, and Alireza Gharabaghi. 2014. Assessing attention and cognitive function in completely locked-in state with event-related brain potentials and epidural electrocorticography. *Journal of Neural Engineering* 11, 2 (Feb. 2014), 026006. https://doi.org/10.1088/1741-2560/11/2/026006

[2] Rute Bettencourt, Miguel Castelo-Branco, Edna Gonçalves, Urbano J. Nunes, and Gabriel Pires. 2024. Comparing Several P300-Based Visuo-Auditory Brain-Computer Interfaces for a Completely Locked-in ALS Patient: A Longitudinal Case Study. *Applied Sciences* 14, 8 (April 2024), 3464. https://doi.org/10.3390/app14083464

[3] Rodrigo Brito, Adriana Baltar, Marina Berenguer-Rocha, Lívia Shirahige, Sérgio Rocha, André Fonseca, Daniele Piscitelli, and Kátia Monte-Silva. 2021. Intrahemispheric EEG: A New Perspective for Quantitative EEG Assessment in Poststroke Individuals. *Neural Plasticity* 2021 (Sept. 2021), 1–8. https://doi.org/10.1155/2021/5664647

[4] Ujwal Chaudhary, Ioannis Vlachos, Jonas B. Zimmermann, Arnau Espinosa, Alessandro Tonin, Andres Jaramillo-Gonzalez, Majid Khalili-Ardali, Helge Topka, Jens Lehmberg, Gerhard M. Friehs, Alain Woodtli, John P. Donoghue, and Niels Birbaumer. 2022. Spelling interface using intracortical signals in a completely locked-in patient enabled via auditory neurofeedback training. *Nature Communications* 13, 1 (March 2022). https://doi.org/10.1038/s41467-022-28859-8

[5] Michele Angelo Colombo, Martino Napolitani, Melanie Boly, Olivia Gosseries, Silvia Casarotto, Mario Rosanova, Jean-Francois Brichant, Pierre Boveroux, Steffen Rex, Steven Laureys, Marcello Massimini, Arturo Chieregato, and Simone Sarasso. 2019. The spectral exponent of the resting EEG indexes the presence of consciousness during unresponsiveness induced by propofol, xenon, and ketamine. *NeuroImage* 189 (April 2019), 631–644. https://doi.org/10.1016/j.neuroimage.2019.01.024

[6] Thomas Donoghue, Matar Haller, Erik J. Peterson, Paroma Varma, Priyadarshini Sebastian, Richard Gao, Torben Noto, Antonio H. Lara, Joni D. Wallis, Robert T. Knight, Avgusta Shestyuk, and Bradley Voytek. 2020. Parameterizing neural power spectra into periodic and aperiodic components. *Nature Neuroscience* 23, 12 (Nov. 2020), 1655–1665. https://doi.org/10.1038/s41593-020-00744-x

[7] Simon Finnigan, Andrew Wong, and Stephen Read. 2016. Defining abnormal slow EEG activity in acute ischaemic stroke: Delta/alpha ratio as an optimal QEEG index. *Clinical Neurophysiology* 127, 2 (Feb. 2016), 1452–1459. https://doi.org/10.1016/j.clinph.2015.07.014

[8] Simon P. Finnigan, Michael Walsh, Stephen E. Rose, and Jonathan B. Chalk. 2007. Quantitative EEG indices of sub-acute ischaemic stroke correlate with clinical outcomes. *Clinical Neurophysiology* 118, 11 (Nov. 2007), 2525–2532. https://doi.org/10.1016/j.clinph.2007.07.021

[9] Brandon Foreman and Jan Claassen. 2012. Quantitative EEG for the detection of brain ischemia. *Critical Care* 16, 2 (2012), 216. https://doi.org/10.1186/cc11230

[10] Vernon J Lawhern, Amelia J Solon, Nicholas R Waytowich, Stephen M Gordon, Chou P Hung, and Brent J Lance. 2018. EEGNet: a compact convolutional neural network for EEG-based brain–computer interfaces. *Journal of Neural Engineering* 15, 5 (July 2018), 056013. https://doi.org/10.1088/1741-2552/aace8c

[11] Suzanne Martens, Michael Bensch, Sebastian Halder, Jeremy Hill, Femke Nijboer, Ander Ramos-Murguialday, Bernhard Schoelkopf, Niels Birbaumer, and Alireza Gharabaghi. 2014. Epidural electrocorticography for monitoring of arousal in locked-in state. *Frontiers in Human Neuroscience* 8 (Oct. 2014). https://doi.org/10.3389/fnhum.2014.00861

[12] Yoji Okahara, Kouji Takano, Masahiro Nagao, Kiyohiko Kondo, Yasuo Iwadate, Niels Birbaumer, and Kenji Kansaku. 2018. Long-term use of a neural prosthesis in progressive paralysis. *Scientific Reports* 8, 1 (Nov. 2018). https://doi.org/10.1038/s41598-018-35211-y

[13] Gabriel Pires, Urbano Nunes, and Miguel Castelo-Branco. 2011. Statistical spatial filtering for a P300-based BCI: Tests in able-bodied, and patients with cerebral palsy and amyotrophic lateral sclerosis. *Journal of Neuroscience Methods* 195, 2 (Feb. 2011), 270–281. https://doi.org/10.1016/j.jneumeth.2010.11.016

[14] Arianna Secco, Alessandro Tonin, Aygul Rana, Andres Jaramillo-Gonzalez, Majid Khalili-Ardali, Niels Birbaumer, and Ujwal Chaudhary. 2020. EEG power spectral density in locked-in and completely locked-in state patients: a longitudinal study. *Cognitive Neurodynamics* 15, 3 (Oct. 2020), 473–480. https://doi.org/10.1007/s11571-020-09639-w

[15] Tomko Settgast, Federico Zilio, Andrea Kübler, and Georg Northoff. 2023. Correlation between Neurophysiological Measures of Consciousness and BCI Performance in a Locked-in Patient. In *2023 11th International Winter Conference on Brain-Computer Interface (BCI)*, Vol. 24. IEEE, 1–6. https://doi.org/10.1109/bci57258.2023.10078703

[16] Shang-Ju Wu, Nicoletta Nicolaou, and Martin Bogdan. 2020. Consciousness Detection in a Complete Locked-in Syndrome Patient through Multiscale Approach Analysis. *Entropy* 22, 12 (Dec. 2020), 1411. https://doi.org/10.3390/e22121411

[17] Federico Zilio, Javier Gomez-Pilar, Ujwal Chaudhary, Stuart Fogel, Tatiana Fomina, Matthis Synofzik, Ludger Schöls, Shumei Cao, Jun Zhang, Zirui Huang, Niels Birbaumer, and Georg Northoff. 2023. Altered brain dynamics index levels of arousal in complete locked-in syndrome. *Communications Biology* 6, 1 (July 2023). https://doi.org/10.1038/s42003-023-05109-1